

# Thermoelectric properties of $\text{CH}_3\text{NH}_3\text{PbI}_3$ investigated using density functional theory and Boltzmann transport calculations

Ibrahim O. A. Ali<sup>1,2</sup>, Daniel P. Joubert<sup>1</sup>, and Mohammed S. H. Suleiman<sup>1,3</sup>

<sup>1</sup> The National Institute for Theoretical Physics, School of Physics and Mandelstam Institute for Theoretical Physics, University of the Witwatersrand, Johannesburg, Wits 2050, South Africa.

<sup>2</sup> Department of Scientific Laboratories, Sudan University of Science and Technology, Khartoum, Sudan.

<sup>3</sup> Department of Basic Sciences, Imam Abdulrahman Bin Faisal University, Dammam, KSA.

E-mail: [ibrphysics@gmail.com](mailto:ibrphysics@gmail.com)

**Abstract.** Mixed organometal perovskite  $\text{CH}_3\text{NH}_3\text{PbI}_3$  has recently emerged as a promising candidate for low cost, high-efficiency solar cells. The materials thermoelectric properties which are key to the solar thermoelectric applications have not been investigated extensively. In this paper, the thermoelectric properties of organic-inorganic halide perovskite  $\text{CH}_3\text{NH}_3\text{PbI}_3$  were studied by solving the semiclassical Boltzmann transport equation on top of density functional theory calculations using maximally-localised Wannier functions (MLWFs). Electronic transport properties were evaluated within the constant relaxation time approximation at four different temperatures 300 K, 500 K, 700 K, and 900 K. The electrical conductivity ( $\sigma$ ) was found to be almost constant in the investigated temperature range, while the Seebeck coefficient ( $S$ ) was found to decrease with increasing temperature and the electronic thermal conductivity ( $\kappa_e$ ) was found to increase with increasing temperature. Theoretical results for the power factor ( $S^2\sigma$ ) and the figure of merit ( $ZT$ ) are analysed. The highest predicted average figure of merit is found to be over 0.8 at 900 K.

## 1. Introduction

Organic-inorganic perovskites  $\text{ABI}_3$  ( $\text{A} = \text{CH}_3\text{NH}_3$  or  $\text{NH}_2\text{CHNH}_2$ ;  $\text{B} = \text{Sn, Pb}$ ), have been specified as light harvesting materials [1]. In addition, they were treated as new thermoelectric materials with a large Seebeck coefficient and low thermal conductivity [2, 3], bring to light that these materials might be potential candidates for thermoelectric applications [4]. The efficiency of thermoelectric devices is characterized by a dimensionless figure of merit  $ZT = S^2\sigma T/\kappa$ , where  $S$ ,  $\sigma$ ,  $T$  and  $\kappa$  refer to Seebeck coefficient, electrical conductivity, temperature and total thermal conductivity, respectively [5]. Both phonons and electrons are heat carriers, therefore the total thermal conductivity has two contributions, the lattice thermal conductivity component  $\kappa_l$  and the electronic thermal conductivity component  $\kappa_e$ . Thermoelectric materials with a large thermoelectric figure of merit ( $ZT$ ) can convert heat to electricity via the Seebeck effect. To have a large figure of merit one needs a large power factor  $S^2\sigma$  and low thermal conductivity  $\kappa$ . In the present work, we studied the thermoelectric properties of the  $\text{CH}_3\text{NH}_3\text{PbI}_3$  in an

orthorhombic system from a combination of semiclassical Boltzmann transport equation and density functional theory calculations using maximally-localised Wannier functions (MLWFs). Section 2 describes the methodology used in the investigation. Section 3 presents the results and discussion. Finally, we shall give our conclusion in section 4.

## 2. Methodology

In this work, the investigation of the electronic structure properties was performed using the Vienna Ab-initio Simulation Package (VASP) [6, 7] based on Density Functional Theory (DFT) [8, 9]. The Projector-Augmented Wave (PAW) [10] method was employed to treat electron-ion interactions. To describe the electrons exchange and correlation effects, we used the Generalized Gradient Approximation (GGA) as parameterized and revised by Perdew, Burke and Ernzerhof (PBEsol)[11].  $4 \times 4 \times 2$  Monkhorst-Pack meshes were used in sampling the Brillouin zone with an energy cut-off of 520 eV. The atomic positions were fully optimized until all components of the forces were less than 1 meV/atom.

The thermoelectric and electronic transport properties were calculated by solving the semiclassical Boltzmann transport equations in the constant relaxation-time approximation (here  $\tau = 10^{-14}$  s) as implemented in the BoltzWann code [12]. The code uses a maximally-localized Wannier functions (MLWFs) [13] basis set to interpolate the bandstructure obtained from the above-mentioned DFT calculations. After using a  $6 \times 4 \times 4$  k-points for the construction of the MLWFs, a  $40 \times 40 \times 40$  was utilized to calculate the electronic transport properties such as Seebeck coefficient  $S$ , electrical conductivity  $\sigma$ , electronic thermal conductivity  $\kappa_e$  and the power factor  $S^2\sigma$ . The computation of MLWFs has been performed within WANNIER90 package [14].

## 3. Results and discussion

### 3.1. Bandstructure and density of states

$\text{CH}_3\text{NH}_3\text{PbI}_3$  is orthorhombic at low temperature (space group Pnma, 62), with the unit cell shown in Figure 1. The bandstructure of the structurally optimized  $\text{CH}_3\text{NH}_3\text{PbI}_3$  was calculated along the high symmetry points of the Brillouin zone (BZ) using the generalized gradient approximation (GGA) for solids (PBEsol). Figure 2 shows the bandstructure obtained from density functional theory (DFT) calculations. The Wannier functions interpolated bandstructure showed excellent agreement with previous first-principles results. The calculated band gap according to PBEsol without including spin orbit coupling was found to be 1.57 eV in good agreement with the experimental results of 1.61 eV [15] and with other theoretical predictions [16, 17]. The total density of states (DOS) and the projected DOS plots calculated for  $\text{CH}_3\text{NH}_3\text{PbI}_3$  are presented in Figure 2.

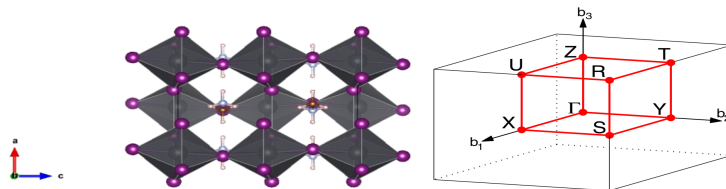


**Figure 1.** (Color online) The crystal structure of orthorhombic  $\text{CH}_3\text{NH}_3\text{PbI}_3$  (left) and its corresponding Brillouin zone (right). Filled red circles are the high symmetry points, while the red bold lines indicate segments of the high symmetry path ( $\Gamma - X - S - Y - \Gamma$ ).

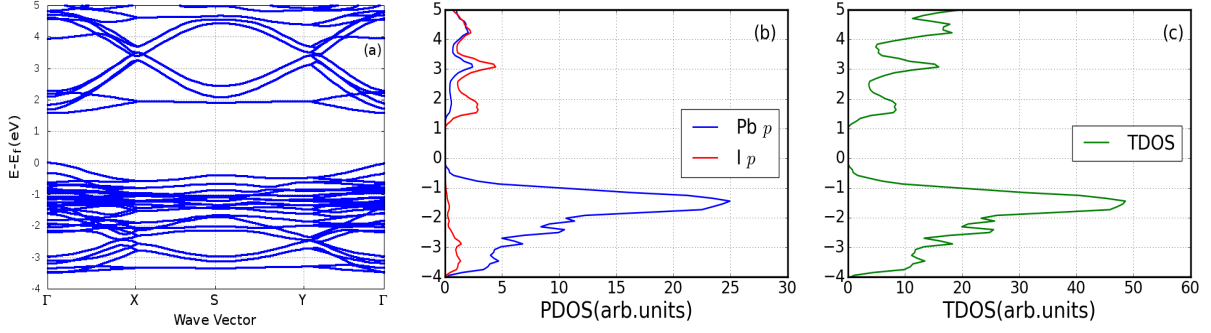


**Figure 2.** (Color online) DFT calculated electronic structure for  $\text{CH}_3\text{NH}_3\text{PbI}_3$ : (a) band structure; (b) partial density of states (PDOS); (c) total density of states (TDOS) using PBEsol.

### 3.2. Thermoelectric properties

The calculated properties are plotted in Figures 3-7 as functions of the chemical potential  $\mu$  at four different temperatures 300 K, 500 K, 700 K and 900 K.

The Seebeck coefficient  $S$ , is defined as the ratio of the electric field to the temperature gradient when the electrical current is zero. The calculated Seebeck coefficients as a function of chemical potential  $\mu$  at different temperatures are presented in Figure 3. From Figure 3 it is clear that Seebeck coefficient of  $\text{CH}_3\text{NH}_3\text{PbI}_3$  has positive values at chemical potential  $\mu = 0$ , indicating that it is a p-type semiconductor. In the  $z$ -direction the maximum values of  $S$  were found to be (2535, 1484, 1062 and 899)  $\mu\text{VK}^{-1}$  at 300 K, 500 K, 700 K and 900 K respectively, which shows that this compound is a good candidate for thermoelectric applications. The absolute value of Seebeck coefficient was found to decrease with increasing temperature.

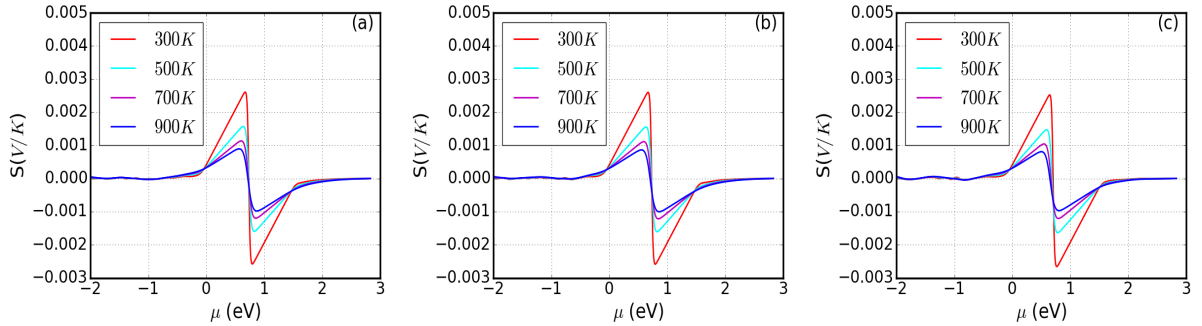


**Figure 3.** (Color online) Variation of Seebeck coefficient with respect to chemical potential at different temperatures in the (a)  $x$ -direction, (b)  $y$ -direction, and (c)  $z$ -direction.

The calculated electrical conductivity  $\sigma$  as a function of chemical potential at different temperatures are presented in Figure 4. Electrical conductivity was found to be almost temperature independent in the considered temperature range. This trend was observed in SnSe[18] and ScRhTe [19]. In general, the value of electrical conductivity increases with increase in absolute value of the chemical potential at all temperatures with the highest value  $4.58 \times 10^6 \Omega^{-1}\text{m}^{-1}$  in the  $z$ -direction at chemical potential 2.84 eV.

The electronic thermal conductivity  $\kappa_e$  as a function of chemical potential at different temperatures is plotted in Figure 5. At chemical potential 2.84 eV the maxima of the electronic thermal conductivity in  $z$ -direction increases from  $33.6 \text{ Wm}^{-1}\text{K}^{-1}$  at 300 K to  $95.68 \text{ Wm}^{-1}\text{K}^{-1}$  at 900 K.

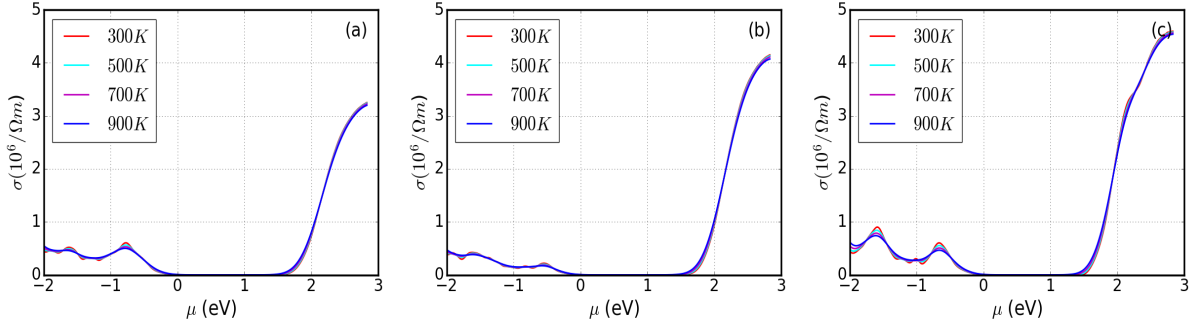


**Figure 4.** (Color online) Variation of electrical conductivity with respect to chemical potential at different temperatures in the (a)  $x$ -direction, (b)  $y$ -direction, and (c)  $z$ -direction.

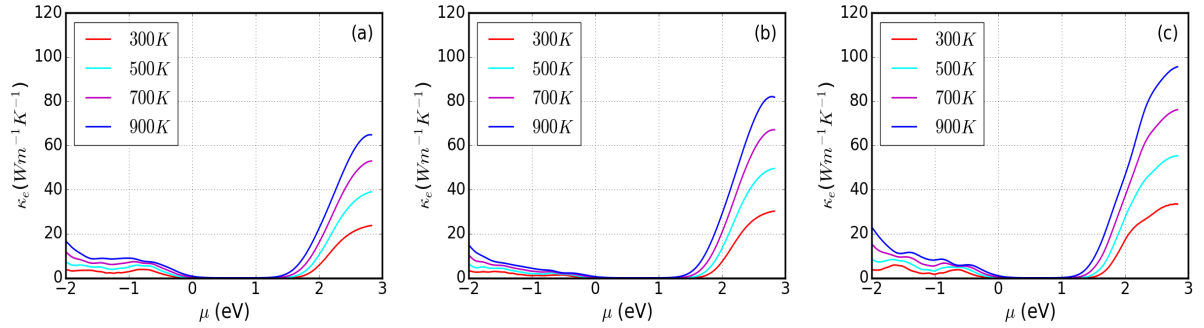


**Figure 5.** (Color online) Electronic thermal conductivity as a function of chemical potential at different temperatures in the (a)  $x$ -direction, (b)  $y$ -direction, and (c)  $z$ -direction.

The power factor  $S^2\sigma$  as a function of chemical potential at different temperatures is shown in Figure 6. The maximum calculated value of the power factor was found to be  $0.013 \text{ Wm}^{-1}\text{K}^{-2}$  in  $z$ -direction at 900 K and chemical potential 1.78 eV.

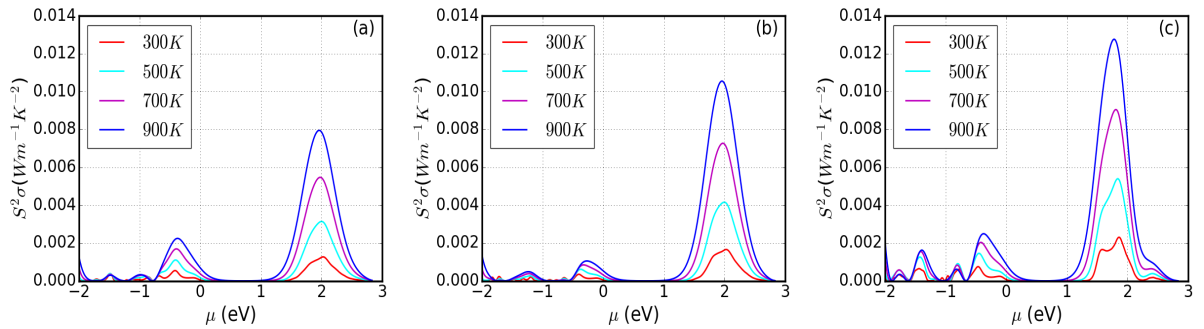


**Figure 6.** (Color online) Calculated power factor as a function of chemical potential at different temperatures in the (a)  $x$ -direction, (b)  $y$ -direction, and (c)  $z$ -direction.

Finally, Figure 7 shows the figure of merit  $ZT$  for  $\text{CH}_3\text{NH}_3\text{PbI}_3$  compound at different temperatures in the  $x$ -,  $y$ - and  $z$ -directions. Figure 7 shows that the maximum value of figure of merit was found to be over 0.8 at 900 K and chemical potential of 1.33 eV, which is a promising value for thermoelectric applications. Typical thermoelectric materials like  $\text{Bi}_2\text{Te}_3$  ( $ZT = 0.8$  at

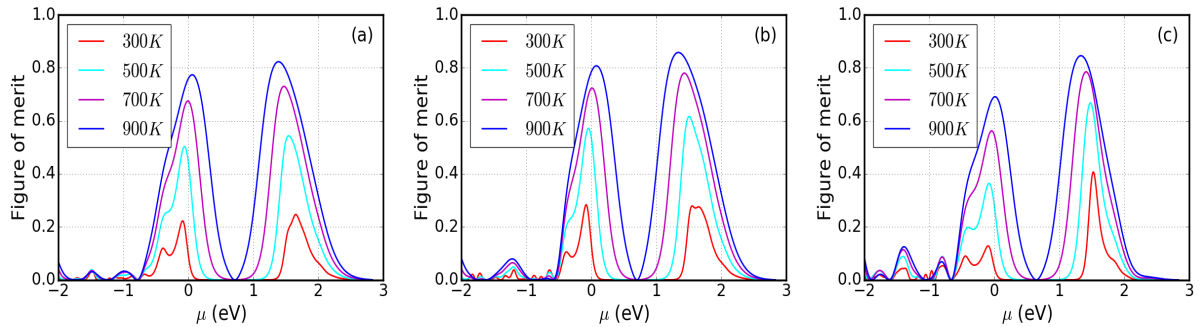


**Figure 7.** (Color online) Calculated figure of merit as a function of chemical potential at different temperatures in the (a)  $x$ -direction, (b)  $y$ -direction, and (c)  $z$ -direction.

300 K) [20] and  $\text{CsBi}_4\text{Te}_6$  ( $ZT = 0.82$  at 225 K) [21, 22] exhibit their maximum  $ZT$  at 300 K and 225 K, respectively, whereas the maximum calculated figure of merit of  $\text{CH}_3\text{NH}_3\text{PbI}_3$  compound appears after 900 K bringing it in the family of PbTe-based middle temperature thermoelectric materials like TI-doped PbTe ( $ZT_{zz} = 0.64$  at 900 K) and Bi-doped PbTe ( $ZT_{xx} = 0.30$  at 900 K) [23], which indicate that our material is optimized at high temperatures.

From the presented figures, it is evident that the obtained Seebeck coefficient (Figure 3) and figure of merit (Figure 7) are nearly isotropic; while the electrical conductivity (Figure 4), the electronic thermal conductivity (Figure 5), and the power factor (Figure 6) are highly anisotropic with their optimal values in the  $z$ -direction.

#### 4. Conclusion

We have carried out a detailed theoretical study of the thermoelectric properties of  $\text{CH}_3\text{NH}_3\text{PbI}_3$  in an orthorhombic system for the first time based on density functional theory combined with the Boltzmann transport theory within the constant relaxation time approximation as implemented in BoltzWann code. Based on the results, we end up with the fact that the perovskite  $\text{CH}_3\text{NH}_3\text{PbI}_3$  can be a good candidate for thermoelectric applications.

#### Acknowledgements

IOAA would like to acknowledge the support he received from NRF-TWAS for funding, and Sudan University of Science and Technology (SUST). We also wish to acknowledge the Centre for High Performance Computing (CHPC), South Africa, for providing us with computing facilities.

#### References

- [1] Lee C, Hong J, Stroppa A, Whangbo M H and Shim J H 2015 *RSC Advances* **5** 78701–78707
- [2] Stoumpos C C, Malliakas C D and Kanatzidis M G 2013 *Inorganic chemistry* **52** 9019–9038
- [3] Pisoni A, Jaćimović J, Barišić O S, Spina M, Gaál R, Forró L and Horváth E 2014 *arXiv preprint arXiv:1407.4931*
- [4] He Y and Galli G 2014 *Chemistry of Materials* **26** 5394–5400
- [5] Goldsmid H, Nolas G and Sharp J 2001 *Thermoelectrics: Basic principles and new materials developments*
- [6] Kresse G and Hafner J 1993 *Physical Review B* **47** 558
- [7] Kresse G and Hafner J 1994 *Physical Review B* **49** 14251
- [8] Hohenberg P and Kohn W 1964 *Physical review* **136** B864

- [9] Kohn W and Sham L J 1965 *Physical review* **140** A1133
- [10] Kresse G and Joubert D 1999 *Physical Review B* **59** 1758
- [11] Perdew J P, Ruzsinszky A, Csonka G I, Vydrov O A, Scuseria G E, Constantin L A, Zhou X and Burke K 2008 *Physical Review Letters* **100** 136406
- [12] Pizzi G, Volja D, Kozinsky B, Fornari M and Marzari N 2014 *Computer Physics Communications* **185** 422–429
- [13] Souza I, Marzari N and Vanderbilt D 2001 *Physical Review B* **65** 035109
- [14] Mostofi A A, Yates J R, Lee Y S, Souza I, Vanderbilt D and Marzari N 2008 *Computer physics communications* **178** 685–699
- [15] Baikie T, Fang Y, Kadro J M, Schreyer M, Wei F, Mhaisalkar S G, Graetzel M and White T J 2013 *Journal of Materials Chemistry A* **1** 5628–5641
- [16] Wang Y, Gould T, Dobson J F, Zhang H, Yang H, Yao X and Zhao H 2013 *Physical Chemistry Chemical Physics* **16** 1424–1429
- [17] Brivio F, Frost J M, Skelton J M, Jackson A J, Weber O J, Weller M T, Goni A R, Leguy A M, Barnes P R and Walsh A 2015 *Physical Review B* **92** 144308
- [18] Wang F Q, Zhang S, Yu J and Wang Q 2015 *Nanoscale* **7** 15962–15970
- [19] Kaur K and Kaur J 2017 *Journal of Alloys and Compounds* **715** 297–303
- [20] Im H J, Kim D H, Mitani T and Je K C 2004 *Japanese journal of applied physics* **43** 1094
- [21] Chung D Y, Hogan T, Schindler J, Iordarridis L, Brazis P, Kannewurf C R, Chen B, Uher C and Kanatzidis M G 1997 Complex bismuth chalcogenides as thermoelectrics *Thermoelectrics, 1997. Proceedings ICT'97. XVI International Conference on (IEEE)* pp 459–462
- [22] Chung D Y, Hogan T P, Rocci-Lane M, Brazis P, Ireland J R, Kannewurf C R, Bastea M, Uher C and Kanatzidis M G 2004 *Journal of the American Chemical Society* **126** 6414–6428
- [23] Borges P, Petersen J, Scolfaro L, Alves H L and Myers T 2015 *Journal of Solid State Chemistry* **227** 123–131